Measurement of calcium isotopes (δ^{44}Ca) using a multicollector TIMS technique

A. Heuser [a,b,*], A. Eisenhauer [a], N. Gussone [a], B. Bock [a], B.T. Hansen [c], Th.F. Nägler [d]

[a] *GEOMAR, Forschungszentrum für Marine Geowissenschaften, Wischhofstr. 1-3, 24148 Kiel, Germany*
[b] *Graduiertenkolleg, Dynamik Globaler Kreisläufe im System Erde, Wischhofstr. 1-3, 24148 Kiel, Germany*
[c] *Göttinger Zentrum für Geowissenschaften, Goldschmidtstr. 3, 37077 Göttingen, Germany*
[d] *Institut für Geologie, Gruppe Isotopengeologie, Universität Bern, Erlacherstr. 9a, 3012 Bern, Switzerland*

Abstract

We propose a new "multicollector technique" for the thermal ionization mass spectrometer (TIMS) measurement of calcium (Ca) isotope ratios improving average internal statistical uncertainty of the ^{44}Ca/^{40}Ca measurements by a factor of 2–4 and average sample throughput relative to the commonly used "peak jumping method" by a factor of 3. Isobaric interferences with potassium (^{40}K$^+$) and titanium (^{48}Ti$^+$) or positively charged molecules like ^{24}Mg^{19}F$^+$, ^{25}Mg^{19}F$^+$, ^{24}Mg^{16}O$^+$ and ^{27}Al^{16}O$^+$ can either be corrected or are negligible. Similar, peak shape defects introduced by the large dispersion of the whole Ca isotope mass range from 40–48 atomic mass units (amu) do not influence Ca-isotope ratios. We use a ^{43}Ca/^{48}Ca double spike with an iterative double spike correction algorithm for precise isotope measurements. (Int J Mass Spectrom 220 (2002) 385–397) © 2002 Elsevier Science B.V. All rights reserved.

1. Introduction

Calcium (Ca) is the fifth most abundant element in the lithosphere and plays a major role in many geological and biological processes (e.g., [1,2]). It has six naturally occurring stable isotopes with atomic mass units (amu) and abundances of ^{40}Ca (96.941%), ^{42}Ca (0.647%), ^{43}Ca (0.135%), ^{44}Ca (2.086%), ^{46}Ca (0.004%) and ^{48}Ca (0.187%). A good overview about previous investigations of possible isotope variations is given by Platzner [3]. Natural variations of the Ca-isotope ratios may be introduced by the beta-decay of the potassium isotope ^{40}K (half-life: 1.277×10^9

years) increasing the relative abundance of ^{40}Ca. The amount of this increase can be used to date igneous and metamorphic rocks [4–8]. Furthermore, Ca-isotope variations can be introduced by kinetic fractionation due to diffusion and chemical exchange reactions. Nägler et al. [9] and Zhu and Macdougall [10] found a temperature dependence of the Ca-isotope fractionation during calcium carbonate ($CaCO_3$) precipitation. These authors observed that with increasing temperatures the heavier isotope (^{44}Ca) becomes enriched relative to ^{40}Ca [9]. However, this temperature controlled fractionation of Ca is different to the behavior of other stable isotope systems like oxygen (δ^{18}O), carbon (δ^{13}O) and boron (δ^{11}O) [11] where the light isotopes become enriched relative to the heavier ones

* Corresponding author. E-mail: aheuser@geomar.de

with increasing temperature. Most likely, the different behavior of Ca during temperature dependent fractionation is related to the fact that Ca is controlled by kinetic fractionation rather than by equilibrium fractionation [12]. This observation confirms measurements by Stahl and Wendt [13] who experimentally showed that the Ca-isotope variations during Rayleigh fractionation must be lower than about 1.5‰/amu. Heumann and Luecke [4] and later O'Neil [14] stated that major Ca-isotope fractionation only occurs when materials with ion exchange capacity are involved and that fractionations are proportional to the mass-difference, that is, δ^{48}Ca is about two times larger than δ^{44}Ca. As a consequence large isotope fractionation effects in an order of up to 22‰ can be observed during ion exchange processes [15–18]. Corless [19] suggested that variations of Ca-isotope ratios in the order up about 10‰ (^{48}Ca/total Ca) can also be caused by kinetic isotope fractionation introduced by biological mediated processes.

It was Russell et al. [20–22] who first used a ^{42}Ca/^{48}Ca double spike for more accurate measurements of the calcium isotopic composition. They normalized the measured ^{44}Ca/^{40}Ca to a calcium fluorite (CaF$_2$) standard supposed to represent average bulk earth composition (δ^{44}Ca $=$ [$(^{44}$Ca/^{40}Ca)$_{sample}$/ $(^{44}$Ca/^{40}Ca)$_{standard}$ $- 1] \times 1000$). Generally, using the "peak jumping method" masses 40, 41, 42, 43, 44 and 48 were measured in sequence on a single Faraday cup. Disadvantage of this time consuming method is the small sample throughput in combination with a reduced internal statistical precision [23]. Other mass spectrometers (diodelaser resonance ionization mass spectrometry [24] and multicollector ICPMS [25]) have also been tested for Ca isotope analysis. The main problem of the ICPMS measurements are isobaric interferences with the argon isotope ^{40}Ar$^+$ on mass 40 or ^{12}C^{16}O$_2$$^+$ on mass 44. Recent progress in the measurement of Ca isotopes using ICP-MS has recently been demonstrated [26–28] by using collision or reaction cells to remove interferering ^{40}Ar$^+$.

Here we present a new technique using a multicollector thermal ionization mass spectrometer (TIMS; Finnigan MAT 262 RPQ+) in combination with a modified double spike technique improving the statistical uncertainties (internal reproducibility) of Ca isotope measurements and the average sample throughput. Multicollector techniques have been used previously for Ca isotope analysis [29,30] but only for measuring masses 40–42 (first sequence) and 42–44 (second sequence) without using a double spike.

2. Experimental methods and mass spectrometry

2.1. ^{43}Ca/^{48}Ca-spike solution

During the mass spectrometric measurement and chemical purification (ion exchange column chemistry and cleaning procedures) of a sample the calcium isotopes fractionate to a large extent [31–34]. In order to measure the original Ca isotope composition before any fractionation introduced by the measurements we apply the Ca double spike technique. This technique was originally introduced for Ca isotope measurements by Russell et al. [21] who used a Ca double spike enriched in ^{42}Ca and ^{48}Ca. In contrast we use a spike enriched in ^{43}Ca and ^{48}Ca being those isotopes with the lowest natural abundance beside ^{46}Ca. A basic request is that the isotope composition of the spike has to be well known and that the spike material is depleted in ^{40}Ca and ^{44}Ca being the isotopes of interest (Table 1).

Table 1
Ca spike concentration and isotope composition

Isotope	Concentration (ng/g)
^{40}Ca	8.86
^{42}Ca	0.46
^{43}Ca	47.20
^{44}Ca	2.91
^{48}Ca	60.0

Isotope ratio	Value
^{40}Ca/^{48}Ca	0.147729
^{42}Ca/^{48}Ca	0.007668
^{43}Ca/^{48}Ca	0.786624
^{44}Ca/^{48}Ca	0.048534
^{44}Ca/^{40}Ca	0.328537

The $^{43}Ca/^{48}Ca$ double spike is added to the sample prior to chemical purification. In the mixture (spike + sample) most of the ^{43}Ca and ^{48}Ca comes from the spike whereas most of the ^{40}Ca and ^{44}Ca is from the sample. From the measured $^{40}Ca/^{48}Ca$ and $^{44}Ca/^{48}Ca$ and the knowledge of the $^{43}Ca/^{48}Ca$ ratio of the spike, we can correct for all not naturally introduced fractionations of the Ca isotopes during chemical purification and mass-spectrometer measurement. Measured $^{44}Ca/^{40}Ca$ ratio have to be corrected for ^{44}Ca and ^{40}Ca introduced by the addition of the Ca spike solution. We adjusted the sample to spike ratio in a way that about 90% of ^{48}Ca and ^{43}Ca originated from the spike. We found that this sample to spike ratio guaranteed most reliable Ca isotope measurements.

2.2. Sample preparation and sample loading

In order to perform the measurements we use three different Ca standards: (1) calcium carbonate powders (NIST SRM915a, Johnson Matthey lot no. 4064 and lot no. 9912, also used by [21]); (2) an international seawater salinity standard (IAPSO); and (3) CaF_2 for the comparison with previous studies and for normalization procedures.

We mixed a Ca standard solution (1) with a concentration of about $500 \, ng_{Ca}/\mu L$ from 250 mg of the NIST SRM915a standard which was dissolved in 4 mL of ultrapure 2N HNO_3 and then further diluted with 196 mL ultrapure H_2O. The Johnson Matthey calcium carbonate standards have been dissolved in ultrapure HCl resulting in concentrations of about $220 \, ng_{Ca}/\mu L$.

Furthermore, a seawater standard solution (2) was mixed from a $100 \, \mu L$ batch of the IAPSO seawater standard and about 12.66 mL of the $^{43}Ca/^{48}Ca$ double spike solution. This mixture was evaporated to dryness and then redissolved in 1 mL of ultrapure 2.5N HCl. Then $500 \, \mu L$ of this solution were loaded onto ion exchange columns (length: 215 mm, diameter: 2 mm; cation exchange resin: BioRad AGW 50 × 8; 200–400 mesh) in order to extract the Ca-fraction. After rinsing the columns with 14 mL 2.5N HCl the Ca-fraction was collected, evaporated and then redissolved in $50 \, \mu L$ 2.5N HCl.

A CaF_2 (3) standard was prepared from a piece of natural fluorite dissolved in 6N HCl and diluted with ultrapure H_2O to a concentration of about $100 \, ng_{Ca}/\mu L$.

For the purpose of mass spectrometric Ca isotope measurements we added $30 \, \mu L$ of the double spike solution to 100 ng of Ca of the sample resulting in a spike to sample ratio of about 1:28. The mixture of spike and sample is evaporated to dryness and then redissolved in $1–2 \, \mu L$ of ultrapure 2.5N HCl in order to guarantee complete chemical equilibrium.

For the TIMS measurements zone refined rhenium ribbon single filaments are used in combination with a Ta_2O_5-activator and the so called "sandwich-technique" following a method previously published by Birck [35]. About $0.5 \, \mu L \, Ta_2O_5$ activator solution is first added on the filament and heated to near dryness at a current of about 0.7 A. Then $1–2 \, \mu L$ sample solution with concentrations of $200–400 \, ng_{Ca}/\mu L$ were added on top of the activator solution and again heated close to dryness at 0.7 A. Another $0.5 \, \mu L$ of the activator were then loaded onto the filament and heated at 0.7 A to dryness. Finally, the filament was heated to 1.5 A and left there for about 20 s. Finally, the electrical current was increased until a weak red glow is visible followed by an immediate shut down of the electrical current. The activator solution stabilizes the signal intensity resulting in a precise measurement of the Ca isotopic composition of the sample/spike mixture.

2.3. TIMS multicollector measurement procedure

All Ca isotope measurements were carried out at the GEOMAR mass spectrometer facilities in Kiel, Germany and at the "Göttinger Zentrum für Geowissenschaften" (Göttingen, Germany). Both institutes are equipped with a Finnigan MAT 262 RPQ+ mass spectrometer which are operated in positive ionization mode with a 10 kV acceleration voltage and a $10^{11} \, \Omega$ resistor for the Faraday cups. The instruments are equipped with nine Faraday cups (2–10) as detection system but cannot account for the
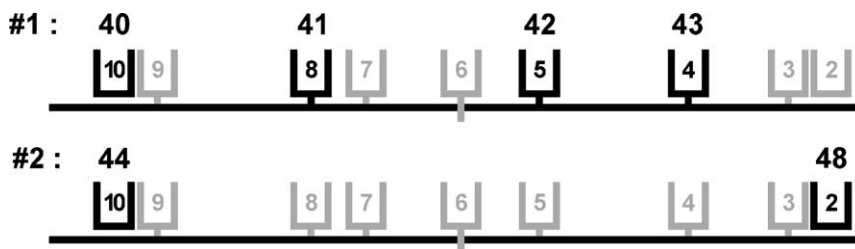
Fig. 1. The cup configuration for Ca isotope measurement on a Finnigan MAT 262 RPQ+ mass spectrometer. In a first sequence $^{40}Ca^+$, $^{41}K^+$, $^{42}Ca^+$ and $^{43}Ca^+$ are measured. In a second sequence $^{44}Ca^+$ and $^{48}Ca^+$ are measured. Cup 6 is a fixed cup. Cup 10 is attached to cup 9 and cup 2 is attached to cup 3.

dispersion of the whole Ca isotope mass range from 40 to 48 amu, respectively.

The Faraday cups are moveable and are arranged in a way to allow the simultaneous measurement of all Ca isotopes in two sequences. During the first sequence (1), the masses of 40, 41, 42 and 43 are measured simultaneously and during the second sequence (2), the masses 44 and 48 are measured separately (Fig. 1, Table 2). Note that with this arrangement of the cups it is also possible to measure the low intensity of $^{46}Ca^+$ in the second sequence using the ion counting system. Mass 41 is measured in order to monitor interfering $^{40}K^+$ ($^{40}K/^{41}K = 1.7384 \times 10^{-3}$).

To start the measurement, the filament is heated automatically to 2800 mA (corresponding to a temperature of about 1450 °C) at a rate of 200–240 mA/min. While heating up a cup gain calibration was carried out. After this first heating the signal was focussed and peak centering was performed. Then the filament was heated manually up to about 3100 mA (corresponding to about 1500–1580 °C). When the intensity of the ion beam reached $3–5 \times 10^{-11}$ A on mass 40, data acquisition was started (temperatures at this point usually are 1500 to about 1600 °C). Before each block the baseline was recorded with closed beam valve (16 s integration time). Data acquisition summarizes 11 scans to one block. A minimum of six blocks corresponding to 66 scans was measured. Data acquisition was normally stopped when the 2σ-standard deviation ($2\sigma_{mean}$) of the $^{44}Ca/^{48}Ca$ and $^{40}Ca/^{48}Ca$ ratios was lower than 0.15‰.

A set of experiments were performed to find the ideal integration and idle times. The integration and idle times have been varied between 1 and 8 s. The

Table 2
Cup positions for Ca isotope multicollector measurements

Cup number	Distance from the center cup (mm)		Mass	
	GEOMAR, Kiel	GZG, Göttingen	First sequence	Second sequence
2	+28.36	+30.15	–	48
3	+25.15	+26.94	–	–
4	+19.07	+19.41	43	–
5	+3.15	+3.58	42	–
6	0	0	–	–
7	−10.42	−9.46	–	–
8	−12.23	−12.83	41	–
9	−25.33	−25.42	–	–
10	−27.17	−28.29	40	44

Note: differences in cup positions between the two spectrometers are due to slightly different effective acceleration voltages. At both mass spectrometers cup 10 is attached to cup 9 and cup 2 is attached to cup 3 due to specific requirements. The distances between cups 9 and 10 and cups 2 and 3 are different for both machines. The largest possible distance for the outer cups 10 and 2 is about 30 mm relative to the fix center cup.
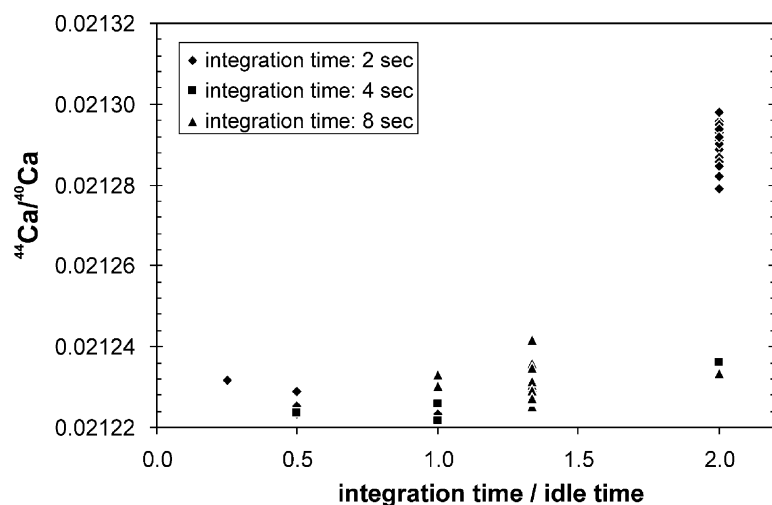
Fig. 2. Set of measurements with different integration times and different integration to idle time ratios. The measurements with a 2 s integration time and 1 s idle time (integration to idle time ratio = 2) show the highest $^{44}Ca/^{40}Ca$ ratios. However, increasing the idle time to 4 s results in lower $^{44}Ca/^{40}Ca$ ratios independent from the ratio of the integration time to idle time.

experiments using 2 s integration and 1 s idle time show the highest $^{44}Ca/^{40}Ca$ ratios while longer integration and idle times result in lower $^{44}Ca/^{40}Ca$ ratios (Fig. 2). Presumably, if the idle time is short (1 s), the ^{40}Ca signal is not completely disintegrated before recording the ^{44}Ca signal. In order to guarantee complete disintegration of the ^{40}Ca signal on the Faraday cup we chose 4 s of integration and idle time for both sequences under measuring conditions. Table 3 shows a summary of the experimental conditions for Ca isotope analysis using TIMS.

2.4. Isobaric interferences and cluster-ions

The most obvious interference on the Ca isotope system arises from $^{40}K^+$ because in all isotope measurements carried out K was present to various extend. The isobaric interference of $^{40}K^+$ interfering with $^{40}Ca^+$ can be corrected by monitoring mass 41 ($^{40}K/^{41}K = 1.7384 \times 10^{-3}$). In general, the intensity on mass 41 is less than 10^{-14} A when measurement started. Thus, an interference correction is negligible because only signals in the order of 10^{-11} A on mass 40 would request a correction.

Further possible isobaric interference arise from magnesium fluoride (MgF^+). These molecular ions would interfere on masses 43 ($^{24}Mg^{19}F^+$) and 44 ($^{25}Mg^{19}F^+$). By monitoring ($^{26}Mg^{19}F^+$) at mass 45

Table 3
Experimental conditions used for Ca isotope analysis by TIMS

Property	Setting
Accelerating voltage	10 kV
Amplifier resistor	$10^{11}\ \Omega$
Source vacuum	$4\text{–}8 \times 10^{-8}$ mbar
Analyzer vacuum	$5\text{–}9 \times 10^{-9}$ mbar
Reference cup	10
Cup gain calibration	Before each sample
Baseline	Each block
	Delay time: 10 s
	Integration time: 16 s
	Closed valve
Peak centering	Every third block
Data collection	Blocks per run: ≥6
	Scans per block: 11
	Integration time: 4 s
	(both sequences)
	Idle time: 4 s (both sequences)
Analyzing temperature	1500–1580 °C

detailed studies indicated no significant isobaric contributions on $^{43}Ca^+$ and $^{44}Ca^+$, respectively. Another group of isobaric interferences may arise from Mg- and Al-oxides interfering on mass 40 ($^{24}Mg^{16}O^+$) and 43 ($^{27}Al^{16}O^+$). These interferences cannot be monitored. However, Mg/Ca and Al/Ca ratios are generally low in our samples, therefore we consider possible interferences to be negligible. Interferences from $^{48}Ti^+$ and double charged $^{84}Sr^{2+}$, $^{86}Sr^{2+}$ and $^{88}Sr^{2+}$ (masses 42, 43 and 44) were not observed.

Whereas no MgF^+ has been observed some other fluorides like CaF^+ (masses 59–67), SrF^+ (masses 103–107) and BaF^+ (masses 152–157) have been detected. The highest signals of CaF^+ have been observed at temperatures of about 1500 °C with an intensity on mass 59 ($^{40}Ca^{19}F^+$) of about 80×10^{-14} A. Measurements showed that the CaF^+ molecules (masses 61, 62, 63 and 67) decrease in several minutes to background levels which inhibited a quantitative determination of their Ca isotopic composition.

2.5. Peak shape defects

Fletcher et al. [29] reported peak shape defects using a wide-dispersion multicollector mass spectrometer. They showed that the peak shapes from the outer
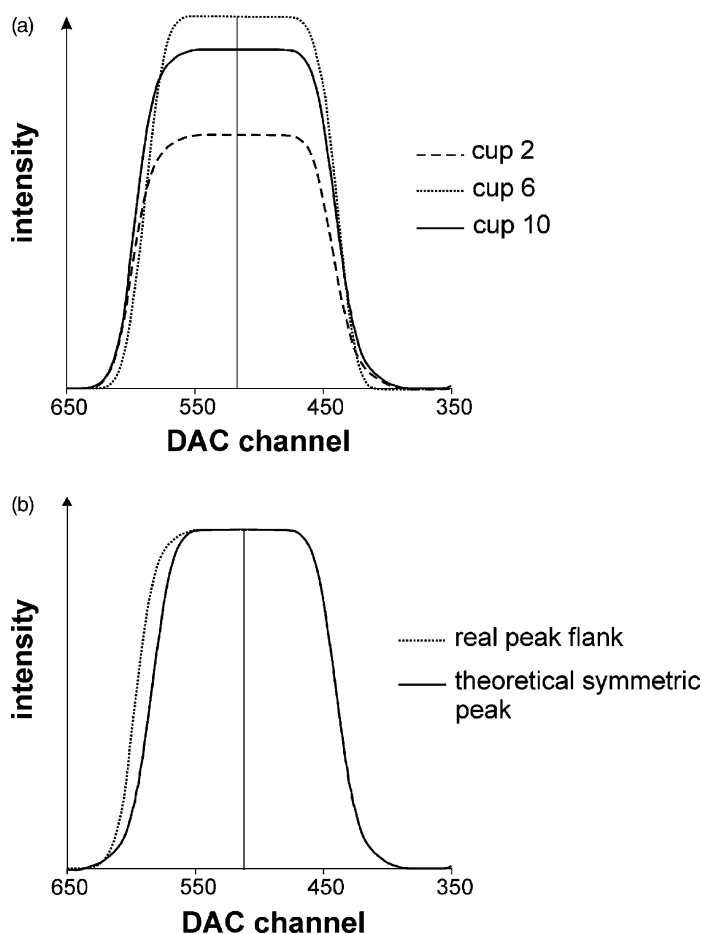

Fig. 3. (a) The peak shapes of cup 6 and of the two outermost cups 2 and 10. It can be seen that the peak shapes of the two outermost cups are asymmetric relative to cup 6. (b) Detailed comparison of expected vs. measured peak shape for cup 10. A peak shape defect can be seen resulting in an asymmetry at the high energy side.

cups are asymmetric limiting the range of measurable mass dispersion. We also found these peak-shape defects for the outer cups (Fig. 3) but the asymmetry is less pronounced than reported by Fletcher et al. [29]. By narrowing the aperture slits the asymmetry of the peak shapes can be reduced. However, measurements with and without the aperture slits do not show any significant influence on the Ca-isotope ratios. Therefore, we conclude that the small peak shape defects observed are negligible.

3. Double spike correction

3.1. Ca double spike data reduction algorithm

The results of the measurements have to be corrected for the added ^{43}Ca/^{48}Ca double spike. We use an iterative routine based on an algorithm presented by Compston and Oversby [36] and originally designed for lead isotope analysis. In this algorithm the linear fractionation terms have been replaced by terms which allow a correction following the exponential law. The use of the exponential law was proposed by Russell et al. [21] and later by Hart and Zindler [37] to be more suitable for fractionation correction of the Ca isotope system (Fig. 5, Eqs. (2) and (8)). The basic ideas are visualized in Fig. 4 where it is schematically illustrated that the measured Ca-isotope ratios of the sample/spike mixture $(^{40}$Ca/^{48}Ca$)_{meas}$, $(^{43}$Ca/^{48}Ca$)_{meas}$, $(^{44}$Ca/^{48}Ca$)_{meas}$ do not plot on the ideal mixing line due to the mixing of spike and sample solution having different Ca isotope composition and due to isotope fractionation during mass spectrometer measurement.

This problem can be solved by an iterative method as it is visualized in the flow chart of Fig. 5. Iterative solutions to the "exponential double spike" problem have also been presented in [9,38,39] based on the routines of Compston and Oversby [36] or other routines (e.g., [40–42]).

The algorithm presented in Fig. 5 starts with a first approximation of the spike to sample ratio Q ($Q = {}^{48}$Ca$_{sample}/^{48}$Ca$_{spike}$). Q can be calculated based on the measured $(^{40}$Ca/^{48}Ca$)_{meas}$ ratio ($Q_{48(40)}$ in
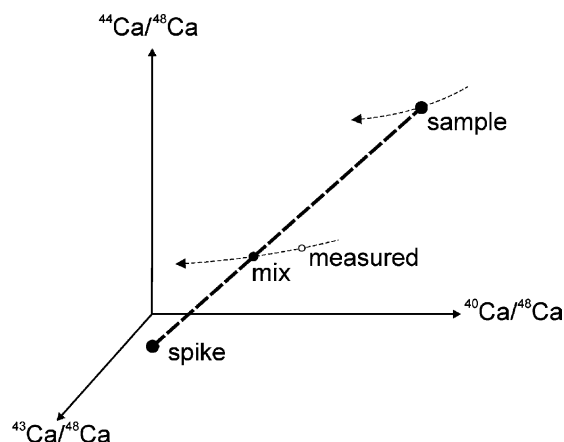

Fig. 4. Schematic three-dimensional illustration of the Ca isotope composition of the spike, sample and the spike/sample mixture. Dotted lines represent fractionation curves. The values of the "mix" point has to be calculated from the "measured" point by an iterative approach. For calculation the well known Ca-isotope ratios of the "spike" are used and for the "sample" ratios as start parameters the previously published values of Russell et al. [21] are adopted.

Eq. (11)) and from the $(^{44}$Ca/^{48}Ca$)_{meas}$ ratio ($Q_{48(44)}$ in Eq. (12)). Note that the $(^{40}$Ca/^{48}Ca$)_{sample}$ and $(^{44}$Ca/^{48}Ca$)_{sample}$ values in Eqs. (11) and (12) for this first cycle of the algorithm correspond to either the $(^{40}$Ca/^{48}Ca$)$ and $(^{44}$Ca/^{48}Ca$)$ of a Ca standard or to the measured $(^{40}$Ca/^{48}Ca$)$ and $(^{44}$Ca/^{48}Ca$)$ of the unspiked sample. Of course, calculated $Q_{48(40)}$ and $Q_{48(44)}$ are different but serve as base for the first approximation (Eq. (1)) of the ^{43}Ca/^{48}Ca ratio $(^{43}$Ca/^{48}Ca$)_{calc}$. Q_{48} is the arithmetic mean of $Q_{48(44)}$ and $Q_{48(40)}$ (Eq. (13)). Then, a first approximation of the fractionation factor β can be estimated (Eq. (2)) from the calculated $(^{43}$Ca/^{48}Ca$)_{calc}$ and the measured $(^{43}$Ca/^{48}Ca$)_{meas}$ ratios. From Eqs. (3) and (4) fractionation factor β allows to calculate improved values of $(^{40}$Ca/^{48}Ca$)_{calc}$, $(^{44}$Ca/^{48}Ca$)_{calc}$ from $(^{40}$Ca/^{48}Ca$)_{meas}$ and $(^{44}$Ca/^{48}Ca$)_{meas}$. In Eq. (5) a first approximation $(^{44}$Ca/^{40}Ca$)_{calc}$ and from Eq. (7) a first estimate of the anticipated $(^{44}$Ca/^{40}Ca$)_{sample-new}$ can be calculated. Comparison of $(^{44}$Ca/^{40}Ca$)_{sample}$ and $(^{44}$Ca/^{40}Ca$)_{sample-new}$ in Eq. (8) allows the calculation of a fractionation factor (fu) and a new estimate of the $(^{44}$Ca/^{48}Ca$)_{sample-new}$ ratio (Eq. (9)) and the

(1)
$$\left(\frac{^{43}Ca}{^{48}Ca}\right)_{calc} = \frac{\left(\frac{^{43}Ca}{^{48}Ca}\right)_{spike} + Q_{48}\left(\frac{^{43}Ca}{^{48}Ca}\right)_{sample}}{1+Q_{48}}$$

(2)
$$\beta = \frac{\log\left[\left(\frac{^{43}Ca}{^{48}Ca}\right)_{calc} \Big/ \left(\frac{^{43}Ca}{^{48}Ca}\right)_{meas}\right]}{\log\left(\frac{^{43}Ca}{^{48}Ca}\right)}$$

(3)
$$\left(\frac{^{40}Ca}{^{48}Ca}\right)_{calc} = \left(\frac{^{40}Ca}{^{48}Ca}\right)_{meas} \cdot \left(\frac{40}{48}\right)^{\beta}$$

(4)
$$\left(\frac{^{44}Ca}{^{48}Ca}\right)_{calc} = \left(\frac{^{44}Ca}{^{48}Ca}\right)_{meas} \cdot \left(\frac{44}{48}\right)^{\beta}$$

(5)
$$\left(\frac{^{44}Ca}{^{40}Ca}\right)_{calc} = \frac{\left(\frac{^{44}Ca}{^{48}Ca}\right)_{calc}}{\left(\frac{^{40}Ca}{^{48}Ca}\right)_{calc}}$$

(6)
$$Q_{40} = Q_{48} \cdot \frac{\left(\frac{^{40}Ca}{^{48}Ca}\right)_{sample}}{\left(\frac{^{40}Ca}{^{48}Ca}\right)_{spike}}$$

(7)
$$\left(\frac{^{44}Ca}{^{40}Ca}\right)_{sample-new} = \left[1+\frac{1}{Q_{40}}\right] \cdot \left(\frac{^{44}Ca}{^{40}Ca}\right)_{calc} - \left[\frac{1}{Q_{40}} \cdot \left(\frac{^{44}Ca}{^{40}Ca}\right)_{spike}\right]$$

(8)
$$fu = \frac{\log\left[\left(\frac{^{44}Ca}{^{40}Ca}\right)_{sample-new} \Big/ \left(\frac{^{44}Ca}{^{40}Ca}\right)_{sample}\right]}{\log\left(\frac{44}{40}\right)}$$

(9)
$$\left(\frac{^{44}Ca}{^{48}Ca}\right)_{sample-new} = \left(\frac{^{44}Ca}{^{48}Ca}\right)_{sample} \cdot \left(\frac{44}{48}\right)^{fu}$$

(10)
$$\left(\frac{^{40}Ca}{^{48}Ca}\right)_{sample-new} = \left(\frac{^{40}Ca}{^{48}Ca}\right)_{sample} \cdot \left(\frac{40}{48}\right)^{fu}$$

Start

(11)
$$Q_{48(40)} = \frac{\left(\frac{^{40}Ca}{^{48}Ca}\right)_{meas} - \left(\frac{^{40}Ca}{^{48}Ca}\right)_{spike}}{\left(\frac{^{40}Ca}{^{48}Ca}\right)_{sample} - \left(\frac{^{40}Ca}{^{48}Ca}\right)_{meas}}$$

(12)
$$Q_{48(44)} = \frac{\left(\frac{^{44}Ca}{^{48}Ca}\right)_{meas} - \left(\frac{^{44}Ca}{^{48}Ca}\right)_{spike}}{\left(\frac{^{44}Ca}{^{48}Ca}\right)_{sample} - \left(\frac{^{44}Ca}{^{48}Ca}\right)_{meas}}$$

(13)
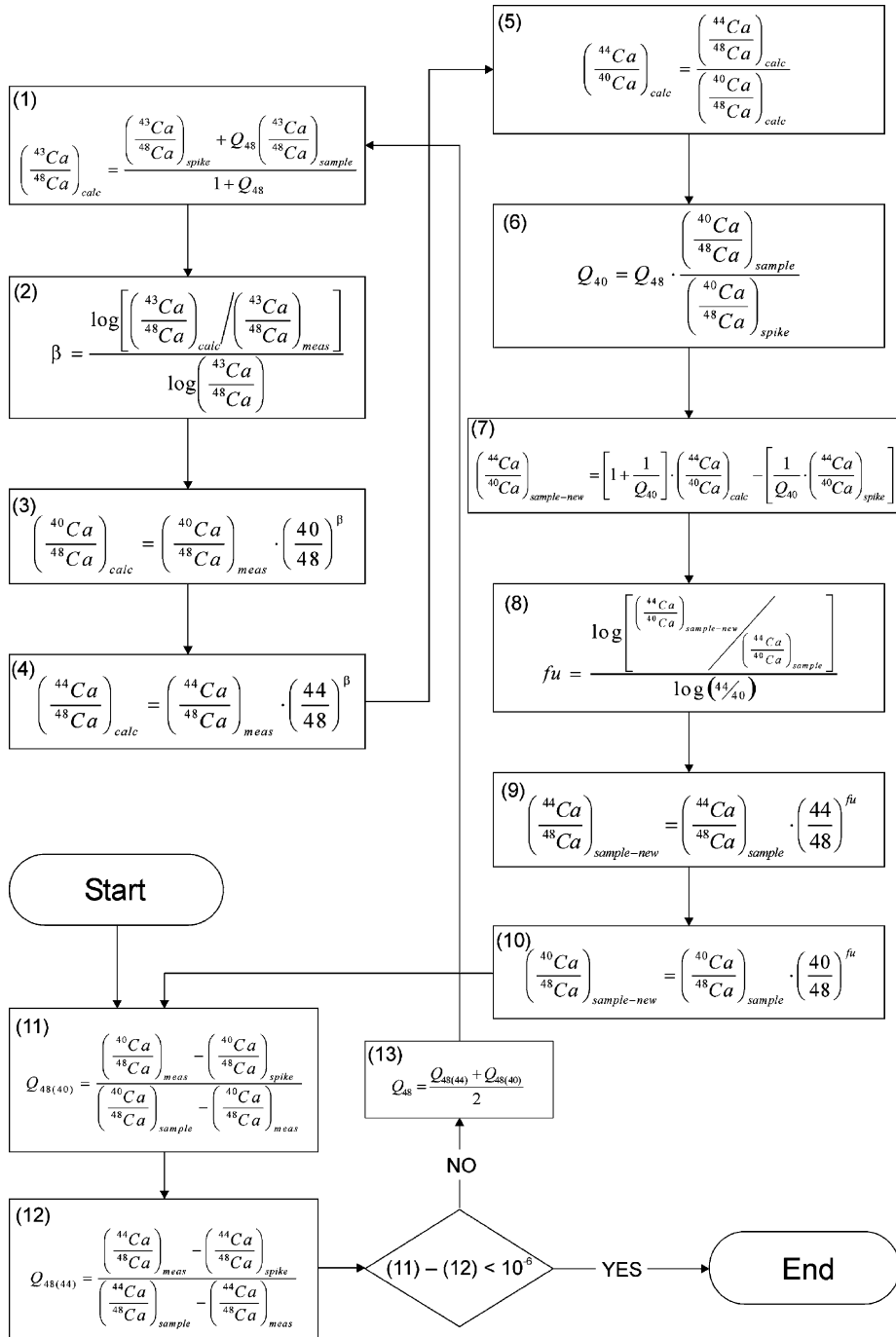$$Q_{48} = \frac{Q_{48(44)} + Q_{48(40)}}{2}$$

NO

$(11) - (12) < 10^{-6}$

YES

End

Fig. 5. Flow chart of the numerical algorithm applied to determine the original $(^{44}Ca/^{40}Ca)_{sample}$ ratio from the $(^{40}Ca/^{48}Ca)_{meas}$ and $(^{44}Ca/^{48}Ca)_{meas}$ ratios. Meas: measured Ca-isotope ratios of the spike/sample mixture; spike: Ca-isotope ratios of the pure spike; sample: Ca-isotope ratios of the pure sample or a standard material; calc: calculated Ca-isotope ratios after first fractionation correction; sample-new: Ca-isotope ratios after a second fractionation correction being the "sample" values for the next cycle.

$(^{40}Ca/^{48}Ca)_{sample\text{-}new}$ ratio (Eq. (10)). With the latter values algorithm will start again at Eqs. (11) and (12). The iterations converge rapidly already after about 4–5 cycles the difference between $Q_{48(40)}$ and $Q_{48(44)}$ becomes lower than about 10^{-6} and iteration can be terminated.

3.2. Start values for the iterative Ca double spike correction

As described in Section 3.1 the values of the $(^{40}Ca/^{48}Ca)_{sample}$, $(^{43}Ca/^{48}Ca)_{sample}$ and $(^{44}Ca/^{48}Ca)_{sample}$ in our double spike correction algorithm can either be the $^{40}Ca/^{48}Ca$, $^{43}Ca/^{48}Ca$ and $^{44}Ca/^{48}Ca$ ratios of a standard or of the unspiked (pure) sample. A set of experiments was performed in order to find an optimal "standard" isotopic composition as starting values for the $(^{40}Ca/^{48}Ca)_{sample}$, $(^{43}Ca/^{48}Ca)_{sample}$ and $(^{44}Ca/^{48}Ca)_{sample}$ for carbonate samples.

Two different batches of the NIST carbonate standard have been prepared, one with a spike to sample ratio about 30% larger (overspiked) than usual and a second batch with a spike to standard ratio about 30% less (underspiked) than usual. All $^{44}Ca/^{40}Ca$ results were calculated using the $^{40}Ca/^{48}Ca$, $^{43}Ca/^{48}Ca$ and $^{44}Ca/^{48}Ca$ isotope ratios published by Russell et al.

[21] ("Russell values") or using the Ca isotope composition published by Moore and Machlan [43] and defined by the IUPAC ("IUPAC values") as the natural Calcium isotope composition [44] (Fig. 6).

The $\delta^{44}Ca$ values for the underspiked (b), the normal spiked (90% of the ^{43}Ca and ^{48}Ca originated from the spike) (a) and the overspiked (c) measurements are in the same range using the "Russell values" ($\delta^{44}Ca \sim -1.3‰$). Using the "IUPAC values" for the normal spiked standard a shift ($\Delta\delta$) of about 0.43‰ towards lighter values is observed. This shift is smaller for the underspiked standard measurements ($\Delta\delta = 0.32‰$) but larger for the overspiked standard measurements ($\Delta\delta = 0.64‰$). Therefore, we suggest to use the Ca-isotope ratios previously published [21] as standard isotopic composition being the start values in our Ca double spike correction algorithm.

4. Results and discussion

4.1. Peak jumping vs. multicollector isotope measurements

In Fig. 7 we compare $^{44}Ca/^{40}Ca$ isotope ratio measurement performed by the common "peak jumping method" with the new "multicollector technique".
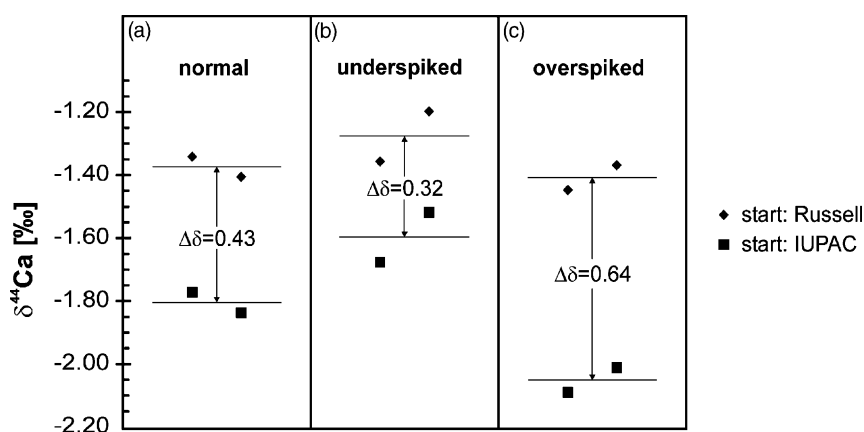

Fig. 6. Calculation of $^{44}Ca/^{40}Ca$ with different starting values for the $(^{40}Ca/^{48}Ca)_{sample}$, $(^{43}Ca/^{48}Ca)_{sample}$, and $(^{44}Ca/^{48}Ca)_{sample}$ in our Ca double spike correction algorithm. Squares represent IUPAC values [44] and diamonds represent the Ca-isotope ratios presented by Russell et al. [21]. In general, the $\delta^{44}Ca$ values based on the IUPAC Ca-isotope ratios tend to be lower than those of the Russell values and show deviations associated with the sample to spike ratio.
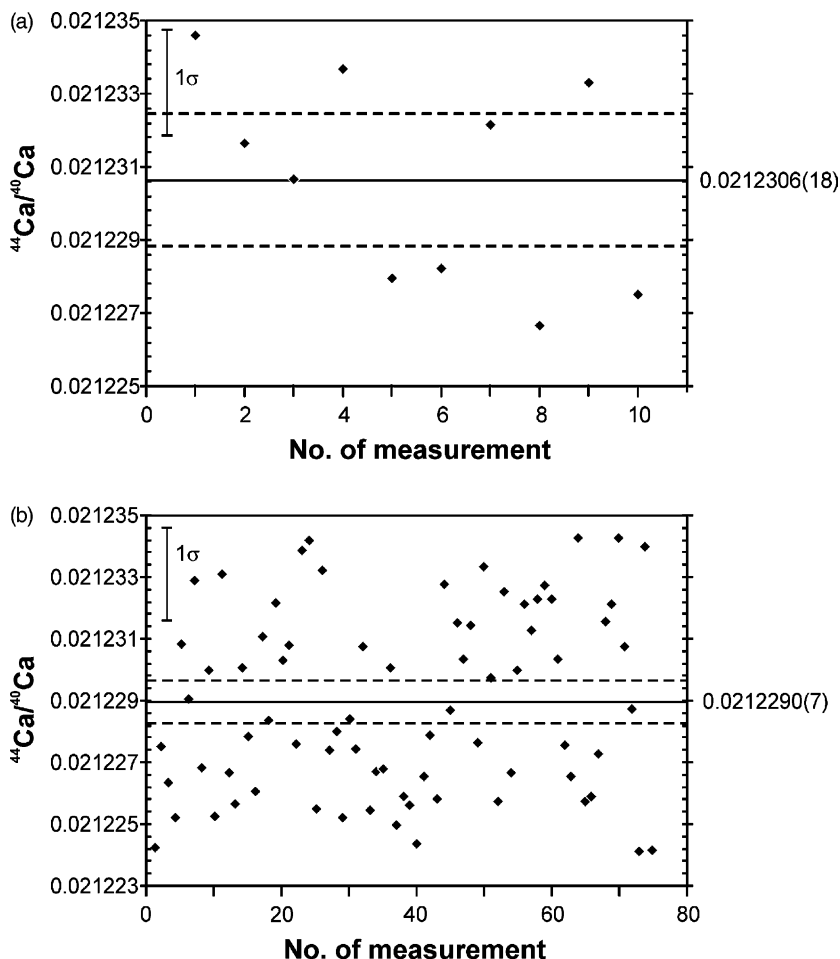
Fig. 7. Comparison of $^{44}Ca/^{40}Ca$ NIST SRM915a measurements performed with the "peak jumping method" (a) and the "multicollector technique" (b). Dotted lines represent 2σ standard deviations of the mean ($2\sigma_{mean}$).

During peak jumping masses 40, 42, 43, 44 and 48 have been measured on a fixed Faraday cup (cup 6) with 4 s integration and 4 s idle times. The baseline was recorded at the end of each block with closed beam valve. Similar to the multicollector method 11 scans have been recorded as a block. Fig. 7 shows the $^{44}Ca/^{40}Ca$ ratio for (a) the "multicollector measurements" and (b) the "peak jumping" measurements of the NIST SRM915a.

We found that the internal reproducibility for the $^{40}Ca/^{48}Ca$ and $^{44}Ca/^{48}Ca$ ratios of a multicup measurement is generally better than about 0.15‰,

whereas for the single cup measurements statistical uncertainties vary to larger extend from 0.090 to 0.304‰. Most likely, the latter observation reflects the enhanced sensitivity of the "peak jumping" method to fluctuations of the beam intensity. Using the "peak jumping method" about three to four samples can be measured during 1 day. However, applying the "multicollector technique" the sample throughput per day is at least three times higher.

The results for the $^{44}Ca/^{40}Ca$ ratio determined by the single cup measurements range from 0.021226 to 0.021235 and the values of the multicup

measurements are in a range from 0.021224 to 0.021235. Within the statistical uncertainty the mean value of the single cup measurements ($^{44}Ca/^{40}Ca$ = 0.0212306(18), $\delta^{44}Ca_{CaF_2}$ = −1.35‰), is in accord with the mean value of the multicup measurements ($^{44}Ca/^{40}Ca$ = 0.0212290(07), $\delta^{44}Ca_{CaF_2}$ = −1.43‰). Note that the mean value calculated from the multicup measurements are more precise because of the larger number of available measurements. The average deviation of one single measurement

from the mean value standard deviation (variance: $1\sigma = 3 \times 10^{-6}$) is similar for both techniques. As our $^{43}Ca/^{48}Ca$ double spike is not calibrated for the determination of the absolute $^{44}Ca/^{40}Ca$ ratio the above values do not represent the true isotopic composition of the NIST SRM915a calcium carbonate standard.

In order to further verify our new multicollector technique we also measured the two Johnson Matthey $CaCO_3$ standards. Using our new technique we were able to confirm earlier results by Russell et al. [21]
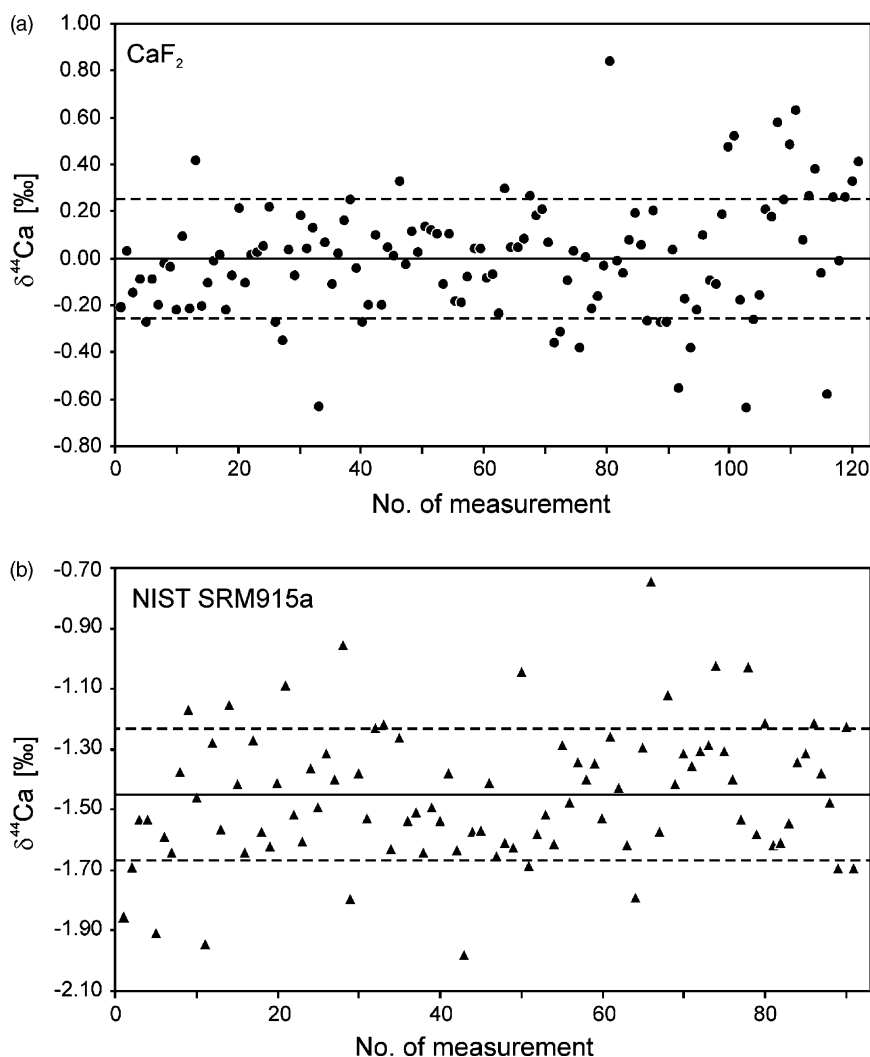

Fig. 8. $\delta^{44}Ca$ values of (a) CaF_2 and (b) NIST SRM915a measurements. Note all $\delta^{44}Ca$ values are normalized to the long-term measurements of the $^{44}Ca/^{40}Ca$ ratio of the CaF_2 standard. Solid lines represent mean $\delta^{44}Ca$ ratios and dashed lines represent the 1σ standard deviation.

that there is a difference of 12‰ between these two standards.

4.2. Reproducibility of $\delta^{44}Ca$

We also used our new multicollector technique for repeated measurements of the CaF_2 standard and the NIST SRM915a carbonate standard. Fig. 8a shows the results of about 120 measurements of CaF_2 and Fig 8b of nearly 90 measurements of the NIST standard. The long-term mean of all $^{44}Ca/^{40}Ca$ measurements of the CaF_2-standard is used for normalization of the $\delta^{44}Ca$ values. The average $\delta^{44}Ca$ value of the CaF_2 measurements is (0.00 ± 0.05)‰ and the $\delta^{44}Ca$ value of the NIST standard is (-1.45 ± 0.05)‰. The given statistical uncertainty represent 2σ deviation of the mean ($2\sigma_{mean}$).

The $\delta^{44}Ca$ values of the CaF_2 have a 1σ standard deviation of 0.25‰. However, the values vary within a relatively wide range between -0.7 and $+0.8$‰. The 1σ standard deviation of the last 30 measurements is 0.35‰ while it is 0.18‰ for the first 90 measurements. The reasons for this pejoration of the external reproducibility remains unclear. Contamination of either the standard solution, the double spike solution or the Ta_2O_5 activator solution should lead to a noticeable shift in the $\delta^{44}Ca$ values in one direction and not to the observed pejoration of the reproducibility.

The range of the $\delta^{44}Ca$ values of the NIST SRM915a measurements vary between -2.0 and -0.8‰. However, the 1σ standard deviation of all measurements is 0.22‰. Opposite to the CaF_2 measurements the range of the $\delta^{44}Ca$ values is not changing significantly during the measurement period. The reason for this is that we did not measure NIST in the time interval we observed the increase in 1σ standard deviation of the CaF_2 measurements.

Acknowledgements

References

[1] R.P. Rubin, G.B. Weiss, J.W.J. Putney, Calcium in Biological Systems, Plenum Publishing Corporation, New York, 1985.
[2] E.T. Degens, Chem. Geol. 25 (1979) 257.
[3] I.T. Platzner, Modern Isotope Ratio Mass Spectrometry, Wiley, Chichester, 1997.
[4] K. Heumann, W. Luecke, Earth. Planet. Sci. Lett. 20 (1973) 341.
[5] K. Heumann, H. Klöppel, Z. Naturforsch. 34b (1979) 1044.
[6] B.D. Marshall, L.J. DePaolo, Geochim. Cosmochim. Acta 46 (1982) 2537.
[7] B.D. Marshall, L.J. DePaolo, Geochim. Cosmochim. Acta 53 (1989) 917.
[8] T.F. Nägler, I.M. Villa, Chem. Geol. 169 (2000) 5.
[9] T.F. Nägler, A. Eisenhauer, A. Müller, C. Hemleben, J. Kramers, Geochem. Geophys. Geosyst. 1 (2000) 2000GC000091.
[10] P. Zhu, J. Macdougall, Geochim. Cosmochim. Acta 62 (1998) 1691.
[11] N. Gussone, A. Eisenhauer, A. Heuser, M. Dietzel, B. Bock, F. Böhm, H. Spero, D.W. Lea, J. Bijma, R. Zeebe, T.F. Nägler, Geochim. Cosmochim. Acta, submitted for publication.
[12] J.R. O'Neil, R.N. Clayton, T.K. Mayeda, J. Chem. Phys. 31 (1969) 5547.
[13] W. Stahl, L. Wendt, Earth. Planet. Sci. Lett. 5 (1968) 184.
[14] J.R. O'Neil, in: J.W. Valley, J.R. O'Neil, H.P. Taylor (Eds.), Reviews of Mineralogy. Stable Isotopes in High Temperature Geological Processes, Mineralogical Society of America, 1986, p. 561.
[15] K. Heumann, Z. Naturforsch. 27b (1972) 492.
[16] K. Heumann, H.-P. Schiefer, Angew. Chem. Int. Ed. 19 (1980) 406.
[17] K. Heumann, H.-P. Schiefer, Z. Naturforsch. 36b (1981) 566.
[18] W.A. Russell, D.A. Papanastassiou, Anal. Chem. 50 (1978) 1151.
[19] J. Corless, Earth. Planet. Sci. Lett. 4 (1968) 475.
[20] W. Russell, D. Papanastassiou, T. Tombrello, S. Epstein, Geochim. Cosmochim. Acta Suppl. 8 (1977) 3791.
[21] W.A. Russell, D.A. Papanastassiou, T.A. Tombrello, Geochim. Cosmochim. Acta 42 (1978) 1075.
[22] W.A. Russell, D.A. Papanastassiou, Anal. Chem. 50 (1978) 1151.
[23] J.L. Skulan, D.J. DePaolo, T.L. Owens, Geochim. Cosmochim. Acta 61 (1997) 2505.

[24] K. Wendt, K. Blaum, B.A. Bushaw, F. Juston, W. Nörtershäuser, N. Trautmann, B. Wiche, Fresen. Z. Anal. Chem. 359 (1997) 361.

[25] L. Halicz, A. Galy, N. Belshaw, R. O'Nions, J. Anal. Atom. Spectrosc. 14 (1999) 1835.

[26] V.I. Baranov, S.D. Tanner, J. Anal. Atom. Spectrosc. 14 (1999) 1133.

[27] I. Feldmann, N. Jakubowski, D. Stuewer, Fresen. J. Anal. Chem. 365 (1999) 415.

[28] S.F. Boulyga, J.S. Becker, Fresen. J. Anal. Chem. 370 (2001) 618.

[29] I. Fletcher, A. Maggi, K. Rosman, N. Naughton, Int. J. Mass Spectrosc. Ion Process. 163 (1997) 1.

[30] D.R. Nelson, M.T. McCulloch, Chem. Geol. (Isot. Geosci.) 79 (1989) 275.

[31] K. Heumann, K. Lieser, H. Elias, in: K. Ogata, T. Hayakawa (Eds.), Recent Developments in Mass Spectrometry, University of Tokyo Press, Tokyo, 1970.

[32] K. Heumann, K. Lieser, Z. Naturforsch. 27b (1972) 126.

[33] K. Heumann, K. Lieser, Geochim. Cosmochim. Acta 37 (1973) 1463.

[34] K. Heumann, H. Klöppel, G. Sigl, Z. Naturforsch. 37b (1982) 786.

[35] J. Birck, Chem. Geol. 56 (1986) 73.

[36] W. Compston, V. Oversby, J. Geophys. Res. 74 (1969) 4338.

[37] S. Hart, A. Zindler, Int. J. Mass Spectrosc. Ion Process. 89 (1989) 287.

[38] C. Siebert, T.F. Nägler, J.D. Kramers, Geochem. Geophys. Geosyst. 2 (2001) 2000GC000124.

[39] M.F. Thirlwall, Chem. Geol. 184 (2002) 255.

[40] B. Hamelin, G. Manhes, F. Albarede, C.J. Allègre, Geochim. Cosmochim. Acta 49 (1985) 173.

[41] N. Gale, Chem. Geol. 6 (1970) 305.

[42] C. Johnson, B. Beard, Int. J. Mass Spectrosc. 193 (1999) 87.

[43] L.J. Moore, L.A. Machlan, Anal. Chem. 44 (1972) 2291.

[44] Commission on Atomic Weights and Isotopic Abundances, Pure Appl. Chem. 70 (1998) 217.